Vibrational Spectroscopy 80 (2015) 66–69

Contents lists available at ScienceDirect

Vibrational Spectroscopy

journal homepage: www.elsevier.com/locate/vibspec

Short communication

# Raman and photoluminescence investigation of CdS/CdSe quantum dots on $TiO_2$ nanoparticles with multi-walled carbon nanotubes and their application in solar cells

Kun-Mu Lee[a,b], Sheng Hsiung Chang[a,*], Ming-Chung Wu[c], Chun-Guey Wu[a,d,**]

[a] Research Center for New Generation Photovoltaics, National Central University, Taoyuan 32001, Taiwan, ROC
[b] Department of Chemical and Material Engineering, National Central University, Taoyuan 32001, Taiwan, ROC
[c] Department of Chemical and Materials Engineering, Chang Gung University, Taoyuan 33302, Taiwan, ROC
[d] Department of Chemistry, National Central University, Taoyuan 32001, Taiwan, ROC

ARTICLE INFO

*Article history:*
Received 20 February 2015
Received in revised form 13 August 2015
Accepted 15 August 2015
Available online 20 August 2015

*Keywords:*
Energy transfer
Raman scattering
Photoluminescence

ABSTRACT

Raman spectroscopy and photoluminescence (PL) were used to investigate the improved short-circuit current density ($J_{SC}$) of CdS/CdSe quantum dot (QD)-sensitized solar cells with multi-walled carbon nanotubes (MWCNTs). Raman and PL experiments were carried out in order to explore the hot-electron and cold-electron injections, respectively. The experimental results showed that the concentration of MWCNTs influences the hot-electron and cold-electron injections from CdS/CdSe QDs to $TiO_2$ nanoparticles. Therefore, the improved $J_{SC}$ in CdS/CdSe QD-sensitized solar cells can be explained as due to the better electron injections.

© 2015 Elsevier B.V. All rights reserved.

## 1. Introduction

Quantum dots have been widely used in solar cells to absorb the sunlight for photocurrent generation [1–4]. Time-resolved second harmonic spectroscopy has been used to demonstrate the efficient hot-electron injection from PbSe nanocrystals to $TiO_2$ nanoparticles [5]. Compared with the use of organic dyes in dye-sensitized solar cells (DSSCs), QDs present higher extinction coefficients [6], and their absorption bandgap can be adjusted by varying the size of the QDs due to the quantum confinement effect [7]. The fabrication process of QDs is also easier than that of organic dyes, which brings a benefit to reach the aim of low-cost solar energy. Cascade QDs have been used to increase the power conversion efficiency (PCE) of QD-SSCs, using materials such as CdS/CdTe, CdS/CdSe, ZnSe/CdSe, and ZnSe/CdSe/ZnSe [4,8–10]. $TiO_2$ nanoparticles [11,12] and ZnO nanostructures [1,2,4] have been widely used as photoanodes. The highest PCE of a QD-SSC is about 6.2% [4], but this is still far lower than the theoretical maximum PCE based on hot- (cold-) electron injection, which is about 43% (32%) [13,14]. Compared with the cold-electron injection from the conduction band of QDs to the Fermi level of the photoanode, the hot-electron injection takes place from QDs to the photoanode at the higher energy level, which results in a larger open-circuit voltage ($V_{OC}$). The PCE of the QD-SSCs is limited by the low fill factor (FF) due to charge carrier recombination originating from the surface defects of the porous photoanode [15]. The low FF results in a low $V_{OC}$ and low $J_{SC}$ [16]. For the photoanode electrode of QD-SSCs, the best way to reduce (increase) the charge carrier recombination (FF) is to increase the electron mobility of the photoanode by adding highly conductive materials such as carbon nanotubes (CNTs) [17], multi-walled carbon nanotubes (MWCNTs) [18], graphene [19], silver [20], and gold [21]. Static and dynamic photoluminescence quenching experiments have been performed to evaluate the efficiency of cold-electron injection from QDs to the photoanode [1,22,23]. However, efficient cold-electron injection from QDs to the photoanode cannot guarantee a high $J_{SC}$ in QD-SSCs, because both hot-electron and cold-electron injections contribute to the generation of the photocurrent.

In this study, the MWCNTs were added to the $TiO_2$ nanoparticles to increase the PCE of CdS/CdSe QD-SSCs. Raman spectroscopy and photoluminescence (PL) were used to investigate the hot-electron and cold-electron injections from QDs to photoanode with and without MWCNTs, respectively.

## 2. Fabrication of $TiO_2$, $TiO_2$/MWCNT films and QD-SSC devices

The $TiO_2$ paste used for screen-printing in this study was prepared by mixing $TiO_2$ nanoparticles (P90), various concentrations of MWCNTs, ethyl cellulose (EC) and terpineol (anhydrous,

* Corresponding author. Fax: +886 3 4252 897.
** Corresponding author. Fax: +886 3 4252 897.
*E-mail addresses:* shchang@ncu.edu.tw (S.H. Chang), t610002@cc.ncu.eud.tw (C.-G. Wu).

http://dx.doi.org/10.1016/j.vibspec.2015.08.001
0924-2031/© 2015 Elsevier B.V. All rights reserved.

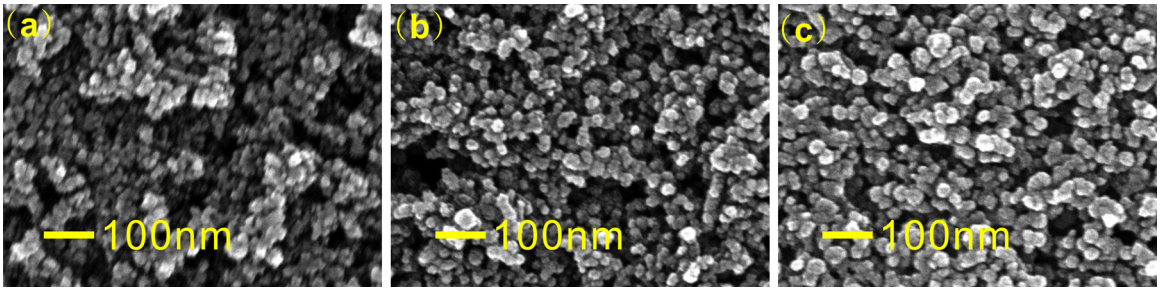


**Fig. 1.** (a), (b), and (c) show images of the surface morphology of $TiO_2$, CdS on $TiO_2$, and CdS/CdSe on $TiO_2$, respectively.

#86480, Fluka). The procedure is described in greater detail as follows: EC (5–15 mPas, #46070, Fluka) and EC (30–70 mPas, #46080, Fluka) were individually dissolved in ethanol to yield a 10 wt% solution, then 1.2 g EC (5–15) and 1.2 g EC (30–70) were added to a flask containing 1.2 g $TiO_2$ nanoparticles (using various concentrations of MWCNTs) and 2.5 terpineol. The paste mixture was dispersed in an ultrasonic bath and a rotary-evaporator was used to remove any residual ethanol or water from the mixture. The final $TiO_2$ paste formula was made with a three-roll mill (EXAKT E50). Screen-printing was used to prepare 4 μm thick $TiO_2$ samples with and without MWCNTs electrodes on fluorine-doped tin oxide (FTO) glass. The active area was fixed at 0.16 $cm^2$. The electrodes were then gradually heated under an $O_2$ gas flow at 450 °C for 30 min to remove any organic materials from the paste. After cooling to room temperature, the mesoporous $TiO_2$ electrodes (photoanodes) were then sequentially sensitized with CdS and CdSe QDs. The CdS layer was deposited on the photoanodes by the successive ion layer absorption and reaction (SILAR) process as previously reported. [24] The CdS loading could be controlled digitally by tuning the number of reaction cycles. Then, CdSe QDs were deposited on the $TiO_2$/CdS structure using the chemical bath deposition (CBD) method. [25] The loading of CdSe QDs can also be controlled by changing the number of reaction cycles. In these studies, two (three) reaction cycles of SILAR (CBD) were used for the deposition of CdS (CdSe). The QD-SSCs were sandwiched together with several parts. [1] Platinum-coated FTO counter electrodes were fabricated by electron-beam evaporation. The internal space of the $TiO_2$ electrodes and Pt counter electrodes was separated by a 60 μm thick hot melting spacer (Surlyn, DuPont), and was filled through a hole with polysulfide electrodes composed of 2 M $Na_2S$, 2 M S, 0.2 M KCl in a mixture of methanol and deionized water (7:3, v/v).

## 3. Measurements and characterizations

For evaluation of the current density–voltage ($J$–$V$) characteristics, a solar simulator (Yamashita Denso, YSS-50S) was used to irradiate the surface of the QD-SSCs, and the data were collected by a Keithley 2400 source meter. The intensity of the simulated sunlight was calibrated by an NREL-certificated Si solar cell (Oriel, 91150V) with a KG-5 filter to an intensity of 100 mW/$cm^2$ (AM 1.5G). The fabricated $TiO_2$ nanoparticles and CdS/CdSe QDs were analyzed by an ultra-high resolution electron microscope (UHR FE-SEM, HITACHI). The results of the hot (cold) electron injection from CdS/CdSe QDs to $TiO_2$ nanoparticles was investigated by a Raman spectroscopy (PL) using a commercial optical microscope system (UniRAM, Protrustech).

## 4. Results and discussion

Fig. 1 presents the surface morphology of the $TiO_2$, CdS on $TiO_2$, and CdSe/CdS on $TiO_2$. CdS and CdSe are coated on the surface of $TiO_2$ nanoparticles, which results in an increase in nanoparticle size as shown in Figs. 1(b) and (c).

The electron injection process is illustrated in Fig. 2. The photogenerated hot electrons in QDs can be injected into $TiO_2$ nanoparticles due to the long hot-electron lifetime (~1 ps) [26]. After the thermalization, the electrons relax to the conduction band of QD. Then, the cold electrons in QDs can be injected into

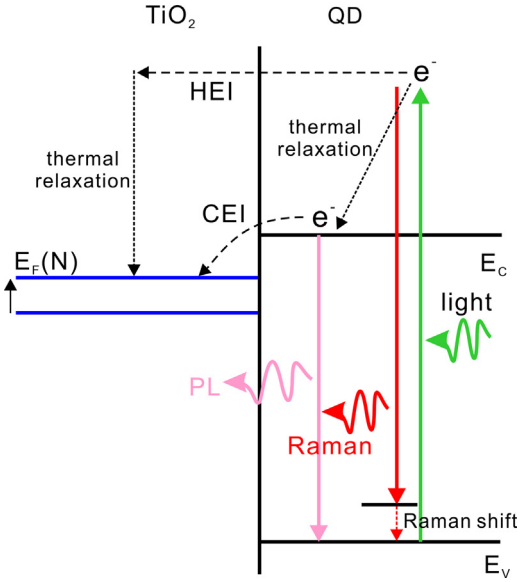


**Fig. 2.** Schematic view of the energy diagram at QD/$TiO_2$ interface. QD: quantum dot; $E_F$: Fermi level; $E_C$: conduction band; $E_V$: valence band; HEI: hot electron injection; CEI: cold electron injection. $E_F$ of $TiO_2$ nanoparticles is proportional to the doping concentration ($N$).

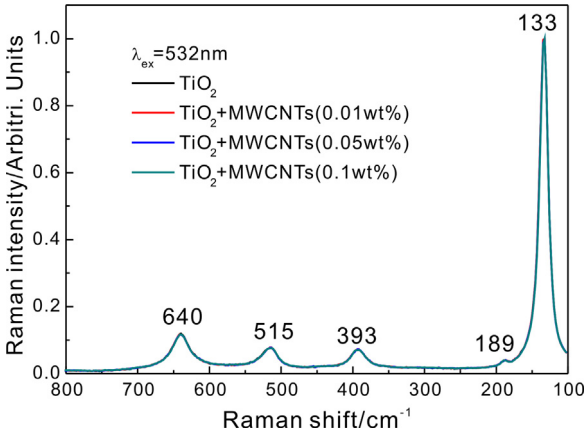


**Fig. 3.** Normalized Raman scattering of $TiO_2$ nanoparticles with different amounts of multi-walled carbon nanotubes.

Download English Version:

https://daneshyari.com/en/article/1250148

Download Persian Version:

https://daneshyari.com/article/1250148

Daneshyari.com